

# Distribution of the ratio of two consecutive level spacings in orthogonal to unitary crossover ensembles

Ayana Sarkar,<sup>\*</sup> Manuja Kothiyal, and Santosh Kumar<sup>†</sup>

*Department of Physics, Shiv Nadar University, Gautam Buddha Nagar, Uttar Pradesh 201314, India*

The ratio of two consecutive level spacings has emerged as a very useful metric in exploring universal features exhibited by complex spectra. It does not require the knowledge of density of states and is therefore quite convenient to compute in studying the spectrum of a general system. The Wigner surmise like results for the ratio distribution are known for the invariant classes of Gaussian random matrices. However, for the crossover ensembles, which are useful in modeling systems with partially broken symmetries, corresponding results have remained unavailable so far. In this work, we derive exact result for the distribution of ratio of two consecutive level spacings in the Gaussian orthogonal to unitary crossover ensemble using a  $3 \times 3$  random matrix model. This crossover is useful in modeling time reversal symmetry breaking in quantum chaotic systems. Although based on a  $3 \times 3$  matrix model, our result can be applied in the study of large spectra also, provided the symmetry breaking parameter facilitating the crossover is suitably scaled. We substantiate this claim by considering Gaussian and Laguerre crossover ensembles comprising large matrices. Moreover, we apply our result to investigate the violation of time-reversal invariance in the quantum kicked rotor system.

## I. INTRODUCTION

Since Wigner's pioneering work in the 1950s, random matrix theory (RMT) has developed into an important field dedicated to the statistical investigation of complex systems. From nuclear physics [1, 2] to finance [3–5], from information and communication theory [6–8] to transport phenomena in mesoscopic systems [9, 10], RMT has found widespread application in a broad range of topics [11–15]. One of the fascinating aspects of RMT is its prediction of certain universal features which are found to be shared by a wide variety of completely unrelated systems. It was conjectured in a seminal work by Bohigas, Giannoni and Schmit that the local fluctuation properties of the spectra of quantum chaotic systems coincide with those of random matrices [16] and there has been an overwhelming evidence in favor of this conjecture [11, 12]. Nearest neighbor spacing distribution (NNSD) is an important and widely studied statistical measure to quantify local fluctuation properties of a given spectrum. As a matter of fact, the agreement of NNSD with the RMT result is considered as a litmus test to indicate that the system under consideration is chaotic.

The NNSD expressions for the classical Gaussian ensembles based on  $2 \times 2$  matrices, famously known as *Wigner surmise*, approximate the corresponding exact results for large matrices very closely and therefore are of immense usefulness in studying spectra of complex systems. Unfortunately, the empirical calculation of NNSD for a general system involves the difficult task of unfolding the spectrum which requires knowledge of the density of states to a very good accuracy, which is not always possible to acquire. Consequently, one seeks alternatives to

NNSD which can be used to quantify the local fluctuation behavior without the need of unfolding. One such quantity is the ratio of two consecutive level spacings and has become quite popular in recent times. In Refs. [17, 18] Atas *et al.* have derived the probability density function of this ratio for the classical Gaussian ensembles belonging to orthogonal, unitary and symplectic invariant classes, and additionally for the Poissonian case which applies to spectra of integrable systems [19]. Although these results are based on  $3 \times 3$  random matrices, similar to the Wigner surmise, they have been found to describe the fluctuation behavior of large spectra to a reasonable accuracy.

The three invariant classes of random matrices mentioned above apply depending on the time-reversal and rotational symmetries exhibited by a system [11–14, 20]. However, there can be instances when the symmetry is *partially broken* and correspondingly the spectra exhibits statistics intermediate between two invariant classes. Such systems can be modeled by crossover random matrix ensembles which can interpolate between two symmetry classes as certain symmetry-breaking or crossover parameter is varied [21–27, 29, 31–37]. The intermediate cases are realized when the crossover parameter assumes a value between its two extremes. This crossover parameter can often be related to some physical quantity while modeling a quantum chaotic system. For instance, application of a weak magnetic field on a mesoscopic system (e.g., a quantum dot) leads to a partial time-reversal invariance violation [9]. Correspondingly, along with the change in spectral behavior, one also observes the effect on electronic transport properties leading to phenomenon such as magnetoconductance [9, 38–42]. In this case, the crossover parameter governing the orthogonal to unitary transition can be related to the magnetic flux. Interestingly, crossover ensembles also find applications in problems where time-reversal and rotation symmetries do not have any direct meaning, for example in multiple channel

---

<sup>\*</sup> ayana1994s@gmail.com

<sup>†</sup> skumar.physics@gmail.com

wireless communication where the crossover is governed by a certain signal-fading parameter [8].

We focus here on an ensemble interpolating between Gaussian Orthogonal Ensemble (GOE) and Gaussian Unitary Ensemble (GUE), and derive exact distribution for the ratio of consecutive level spacings using a  $3 \times 3$  random matrix model. Similar to Wigner surmise, our result can be applied to large dimension cases and to non-Gaussian random matrix ensembles once the crossover parameter is properly scaled. We substantiate this claim by considering interpolating ensembles of Gaussian and Wishart-Laguerre ensembles comprising large matrices. In quantifying the level fluctuation behavior of an arbitrary quantum chaotic system, our result can be applied once the crossover parameter of the RMT model is related to the time-reversal symmetry breaking parameter of the given system. We demonstrate this by investigating the time-reversal symmetry breaking in a quantum kicked rotor (QKR) system [43].

The rest of this paper is organized as follows. In Sec. II we present the random matrix model used for studying the GOE-GUE crossover. In Sec. III we derive the exact result for the ratio distribution using the  $3 \times 3$  case of the matrix model presented in the preceding section. In Sec. IV we examine the scaling behaviour of the crossover parameter for Gaussian ensembles in large dimension cases. Section V deals with the investigation of orthogonal to unitary crossover in Wishart-Laguerre ensemble. In Sec. VI we apply our analytical result for studying the time-reversal symmetry breaking in quantum kicked rotor system. We conclude with a brief summary in Sec. VII.

## II. MATRIX MODEL FOR THE GOE-GUE CROSSOVER

We use the random matrix model proposed by Pandey and Mehta for GOE-GUE crossover [22, 23]:

$$H = \sqrt{1 - \alpha^2} H_1 + \alpha H_2. \quad (1)$$

In this equation,  $H_1$  and  $H_2$  are real-symmetric and complex-Hermitian random matrices with probability densities

$$\mathcal{P}(H_\beta) \propto \exp\left(-\frac{1}{4v^2} \text{tr} H_\beta^2\right), \quad \beta = 1, 2, \quad (2)$$

respectively. The parameter  $v$  appearing above fixes the scale of the problem. Clearly,  $H_1$  and  $H_2$  belong to the GOE and GUE, respectively. The variances of the diagonal and off-diagonal parts (both real and imaginary for GUE) of the Gaussian matrix elements in either case are  $2v^2$  and  $v^2$ , respectively. The matrix model in Eq. (1) interpolates between GOE and GUE as the crossover parameter  $\alpha$  is varied from 0 to 1. Other equivalent forms for the above matrix model are also possible. For example, Lenz and co-workers have considered the random

matrix model [24, 25]

$$H = \frac{1}{\sqrt{1 + \lambda^2}} H_1 + \frac{\lambda}{\sqrt{1 + \lambda^2}} H_2. \quad (3)$$

The relation between parameters  $\alpha$  and  $\lambda$  can be readily established to be  $\alpha = \lambda/\sqrt{1 + \lambda^2}$  or  $\lambda = \alpha/\sqrt{1 - \alpha^2}$ . The parameter  $\lambda$  gives GOE and GUE in the limits 0 and  $\infty$ , respectively. The joint eigenvalue density for the matrix model in Eq. (1) is used in the next section to obtain an exact result for the distribution of ratio of consecutive level spacings.

## III. EXACT RATIO DISTRIBUTION FOR 3-DIMENSIONAL GAUSSIAN MATRICES

Considering the 3-dimensional case, the joint probability density function for the orthogonal-unitary crossover in Gaussian ensemble is given by [22, 23]

$$\begin{aligned} P(x_1, x_2, x_3) &= \frac{1}{48\sqrt{2}\pi v^6 (1 - \alpha^2)^{3/2}} \\ &\times [f(x_1 - x_2) - f(x_1 - x_3) + f(x_2 - x_3)] \\ &\times (x_1 - x_2)(x_2 - x_3)(x_1 - x_3) e^{-\frac{1}{4v^2}(x_1^2 + x_2^2 + x_3^2)}, \end{aligned} \quad (4)$$

where

$$f(u) = \text{erf}\left[\left(\frac{1 - \alpha^2}{8\alpha^2 v^2}\right)^{1/2} u\right], \quad (5)$$

with  $\text{erf}(z) = (2/\sqrt{\pi}) \int_0^z e^{-t^2} dt$  being the error function. The limits  $\alpha \rightarrow 0$  and  $\alpha \rightarrow 1$  in Eq. (4) lead to the joint probability densities of eigenvalues for GOE and GUE, respectively. We have

$$\begin{aligned} P_{\text{GOE}}(x_1, x_2, x_3) &= \frac{1}{48\sqrt{2}\pi v^6} e^{-\frac{1}{4v^2}(x_1^2 + x_2^2 + x_3^2)} \\ &\times |(x_1 - x_2)(x_1 - x_3)(x_2 - x_3)|, \end{aligned} \quad (6)$$

$$\begin{aligned} P_{\text{GUE}}(x_1, x_2, x_3) &= \frac{1}{768\pi^{3/2} v^9} e^{-\frac{1}{4v^2}(x_1^2 + x_2^2 + x_3^2)} \\ &\times [(x_1 - x_2)(x_1 - x_3)(x_2 - x_3)]^2. \end{aligned} \quad (7)$$

For the purpose of computing the desired ratio distribution, we order the eigenvalues such that  $x_1 \leq x_2 \leq x_3$ . The ratio of consecutive level spacings is then given by

$$r = \frac{x_3 - x_2}{x_2 - x_1}. \quad (8)$$

The probability density function of  $r$  can be obtained as

$$\begin{aligned} p(r) &= 3! \int_{-\infty}^{\infty} dx_2 \int_{-\infty}^{x_2} dx_1 \int_{x_2}^{\infty} dx_3 P(x_1, x_2, x_3) \\ &\quad \times \delta\left(r - \frac{x_3 - x_2}{x_2 - x_1}\right). \end{aligned} \quad (9)$$

We proceed similar to Refs. [17, 18] and implement the change of variables  $(x_1, x_2, x_3) \rightarrow (x, x_2, y)$  with  $x = x_2 - x_1$ ,  $y = x_3 - x_2$ . This gives us

$$p(r) = 6 \int_{-\infty}^{\infty} dx_2 \int_0^{\infty} dx \int_0^{\infty} dy P(x_2 - x, x_2, x_2 + y) \times \delta\left(r - \frac{y}{x}\right).$$

On using Eq. (4) we find that in the above expression the variable  $x_2$  appears only in the exponential factor and therefore the integral over it can be trivially performed, leading us to

$$p(r) = \frac{1}{4\sqrt{6\pi} v^5 (1 - \alpha^2)^{3/2}} \int_0^{\infty} dx \int_0^{\infty} dy x y (x + y) \times [f(x) + f(y) - f(x + y)] e^{-\frac{1}{6v^2}(x^2 + xy + y^2)} \delta\left(r - \frac{y}{x}\right). \quad (10)$$

Using the result  $\delta(r - y/x) = x \delta(y - rx)$ , we get rid of the  $y$ -integral and are left with an integration on  $x$  only:

$$p(r) = \frac{r(r+1)}{4\sqrt{6\pi} v^5 (1 - \alpha^2)^{3/2}} \int_0^{\infty} dx x^4 \times [f(x) + f(rx) - f(r+rx)] e^{-\frac{x^2}{6v^2}(r^2 + r + 1)}. \quad (11)$$

The above expression involves three integrals of identical structure which offers an exact result:

$$g(\eta, \zeta) := \frac{4\sqrt{\pi}}{v^5} \int_0^{\infty} dx x^4 \exp\left(-\frac{\eta^2 x^2}{v^2}\right) \operatorname{erf}\left(\frac{\zeta x}{v}\right) = \frac{\zeta(5\eta^2 + 3\zeta^2)}{\eta^4(\eta^2 + \zeta^2)^2} + \frac{3}{\eta^5} \arctan\left(\frac{\zeta}{\eta}\right). \quad (12)$$

Using the above integration result, we obtain the final expression for the probability density function for the ratio of two consecutive level spacings as

$$p(r) = \frac{r(r+1)}{16\sqrt{6}\pi(1-\alpha^2)^{3/2}} [g(a, b) + g(a, br) - g(a, br + b)], \quad (13)$$

where  $g(\eta, \zeta)$  is as given in Eq. (12) and

$$a = \sqrt{\frac{r^2 + r + 1}{6}}, \quad b = \sqrt{\frac{1 - \alpha^2}{8\alpha^2}}. \quad (14)$$

We note that the function  $g(\eta, \zeta)$ , and hence  $p(r)$  is independent of  $v$ . This is expected, as ratio distribution has to be independent of the global scale of the spectrum. This can be seen from Eq. (6) also by considering the scaling  $x \rightarrow vx$ . The three ‘arctan’ terms in  $p(r)$  may be combined to yield a single term, giving us overall

$$p(r) = \frac{r(r+1)}{16\sqrt{6}\pi(1-\alpha^2)^{3/2}} \left[ \frac{b(5a^2 + 3b^2)}{a^4(a^2 + b^2)^2} + \frac{br(5a^2 + 3b^2r^2)}{a^4(a^2 + b^2r^2)^2} - \frac{b(r+1)(5a^2 + 3b^2(r+1)^2)}{a^4(a^2 + b^2(r+1)^2)^2} + \frac{3}{a^5} \arctan\left(\frac{b^3r(r+1)}{a^3 + ab^2(r^2 + r + 1)}\right) \right]. \quad (15)$$

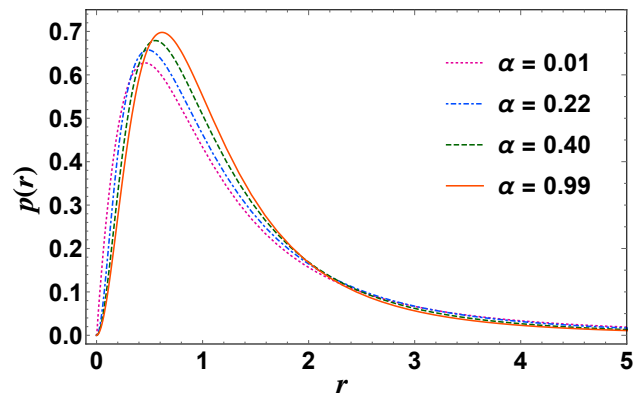


FIG. 1: Distribution of the ratio of two consecutive spacings using Eq. (15) for different  $\alpha$  values.

Equations (13) and (15) may be written in terms of the parameter  $\lambda$  of the matrix model given in Eq. (3) by replacing  $1/(1 - \alpha^2)^{3/2}$  by  $(1 + \lambda^2)^{3/2}$  and  $b$  in Eq. (14) by  $1/(\sqrt{8}\lambda)$ .

In the limit  $\alpha \rightarrow 0$ , we have  $b \rightarrow \infty$ , and therefore  $g(a, b) = g(a, br) = g(a, br + b) = 3\pi/(2a^5)$ . Consequently, we obtain the result for GOE [17, 18]:

$$p_{\text{GOE}}(r) = \frac{27}{8} \frac{r(r+1)}{(r^2 + r + 1)^{5/2}}. \quad (16)$$

Now, for  $\zeta \rightarrow 0$  we obtain  $g(\eta, \zeta) = 8\zeta/\eta^6 - 8\zeta^3/\eta^8 + \mathcal{O}(\zeta^5)$  by invoking the expansion of  $\arctan z$  about  $z = 0$ . Hence, in the limit of  $\alpha \rightarrow 1$  or  $b \rightarrow 0$ , we have

$$g(a, b) + g(a, br) - g(a, br + b) = \frac{8b}{a^6} - \frac{8b^3}{a^8} + \frac{8br}{a^6} - \frac{8b^3r^3}{a^8} - \frac{8(r+1)b}{a^6} + \frac{8(r+1)^3b^3}{a^8} + \mathcal{O}(b^5) = \frac{24r(r+1)b^3}{a^8} + \mathcal{O}(b^5) = \frac{24r(r+1)(1-\alpha^2)^{3/2}}{8^{3/2}a^8} + \mathcal{O}((1-\alpha^2)^{5/2}). \quad (17)$$

This leads to GUE result in the limit  $\alpha \rightarrow 1$  [17, 18]:

$$p_{\text{GUE}}(r) = \frac{81\sqrt{3}}{4\pi} \frac{r^2(r+1)^2}{(r^2 + r + 1)^4}. \quad (18)$$

In Fig. 1 we plot the result in Eq. (15) for probability density function of the ratio of two consecutive levels for three values of  $\alpha$ . The  $\alpha = 0.01$  and  $0.99$  curves are close to GOE and GUE results, while the  $\alpha = 0.22$  and  $0.40$  curves depict intermediate situations. In Fig. 2 we consider  $\alpha = 0.2, 0.7$  and compare analytical result based plots (solid curves) with numerical results (overlaid symbols) obtained from the Monte Carlo simulation of  $3 \times 3$  matrices following the matrix model of Eq. (1). We see an excellent match as we would expect.

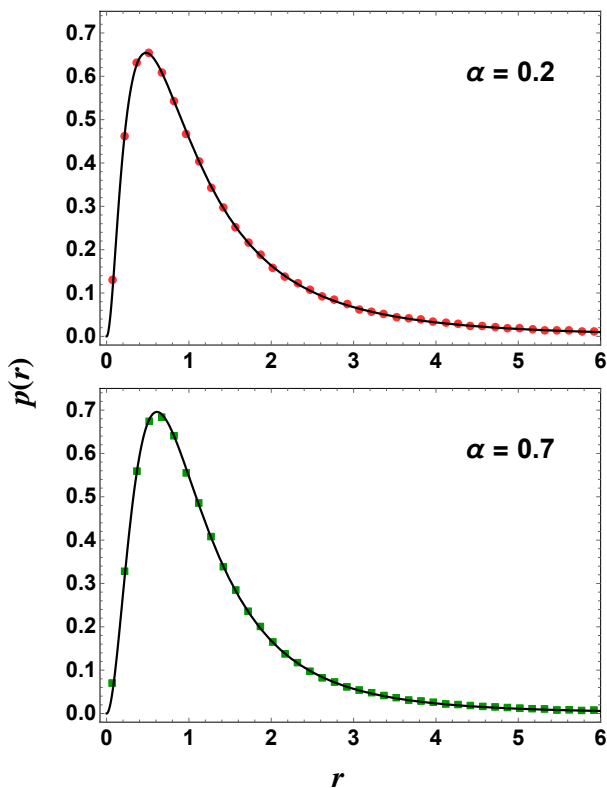


FIG. 2: Comparison between the analytical prediction (solid line) based on Eq. (15) and numerical simulation for ratio distribution in the  $3 \times 3$  case.

#### IV. SCALING OF $\lambda$ FOR LARGE $N$ GAUSSIAN ENSEMBLE

For the invariant cases, i.e.,  $\lambda = 0$  ( $\alpha = 0$ ) and  $\lambda \rightarrow \infty$  ( $\alpha \rightarrow 1$ ), it has been shown that the Wigner-surmise like results, Eqs. (16) and (18), for the ratio distribution work even for large matrix dimension  $N$  [17, 18]. However, for the intermediate cases, we must scale the crossover parameter  $\alpha$  or  $\lambda$  appropriately so that Eq. (15) can be used for large  $N$  also. As a matter of fact, it is known that the transition rate depends on the local density of states or the level density [22, 23, 27–30, 33, 34]. For large  $N$ , the matrix model in Eq. (1) leads to the the Wigner’s semicircular level density

$$R_1(x) = \begin{cases} \frac{1}{\pi} \sqrt{2N - x^2}, & -\sqrt{2N} \leq x \leq \sqrt{2N}, \\ 0, & \text{otherwise,} \end{cases} \quad (19)$$

for the choice  $v^2 = 1/[2(1 + \alpha^2)] = (1 + \lambda^2)/[2(1 + 2\lambda^2)]$ . The effective crossover parameter for small  $\alpha$  is then  $\alpha_{\text{eff}} \sim \alpha R_1(x)$  and equivalently, for small  $\lambda$  we have  $\lambda_{\text{eff}} \sim \lambda R_1(x)$ . This implies that the transition rate is faster in the center of the semicircle. Therefore, although the ratio of consecutive spacings is independent of the local density of states, for the crossover ensemble, the fluctuation behavior of the part of spectrum near at the center is closer to GUE than that near the

edges. We verify this by considering 1000 matrices of size  $N = 1000$  using the matrix model Eq. (3) and numerically obtain the ratio distribution independently using (i) 100 eigenvalues in the center of the spectrum, (ii) 100 eigenvalues comprising 50 and 50 from the left and right edges of the spectrum, and (iii) the entire spectrum. These are displayed in the Fig 3 using histogram stairs of colors red, blue and green, respectively. The extremes corresponding to the GOE and GUE cases based on Eqs. (16) and (18) are shown using gray dotted and orange dashed curves, respectively. For  $\lambda = 0$  all histograms fall on the GOE curve, indicating that everywhere in the spectrum, the fluctuations conform to the orthogonal symmetry. Similarly, for higher values of  $\lambda$ , e.g. 0.08, the histograms more or less coincide with the GUE curve, implying that the crossover is almost complete. However, for intermediate cases the red histogram (spectrum bulk) is closer to the GUE curve than the blue histogram (spectrum edges). This effect can be seen prominently in  $\lambda = 0.02$  and  $0.04$  cases. We also see that for these intermediate cases, the green histogram, which is based on the entire spectrum, is closer to the red histogram. Therefore, the overall behavior is dominated by the bulk and as an approximation we may use the scaling  $\lambda_{\text{eff}} \sim \lambda R_1(0) \sim \sqrt{N}\lambda$  and consider the entire spectrum for examining the local fluctuations. To justify this proposition, based on the matrix model (3), we numerically obtain ratio distributions for matrix dimensions  $N = 100, 500$  and  $1000$  along with several values of  $\lambda$ . These empirical distributions are then fitted with Eq. (15) to obtain the effective crossover parameter  $\lambda_{\text{eff}}$ . The plots of  $\lambda_{\text{eff}}$  vs.  $\sqrt{N}\lambda$  do exhibit linear behavior for small  $\lambda$  values and nearly fall on each other, thereby supporting our deduction above. This scaling was also found to hold in the NNSD expression for the Poisson-GOE crossover studied in Ref. [25].

#### V. APPLICATION TO LAGUERRE ENSEMBLE

In this section, we discuss the orthogonal to unitary crossover in Laguerre ensemble, which is also referred to as Wishart or Wishart-Laguerre ensemble.

Consider  $N \times M$ -dimensional real and complex Ginibre matrices  $A_1$  and  $A_2$ , respectively, from the distributions

$$P_\beta(A_\beta) \propto \exp\left(-\frac{\beta}{2} \text{tr} A_\beta A_\beta^\dagger\right); \quad \beta = 1, 2, \quad (20)$$

where  $\dagger$  represents conjugate-transpose and may be replaced by only transpose ( $T$ ) for  $\beta = 1$ . Considering  $N \leq M$ , the Laguerre Orthogonal Ensemble (LOE) and Laguerre Unitary Ensemble (LUE) comprise the Wishart matrices  $A_1 A_1^T$  and  $A_2 A_2^\dagger$ , respectively. The distribution of ratio of two consecutive level spacings is known from Ref. [18] for  $3 \times 3$  matrix model of Laguerre ensemble in the invariant cases with Laguerre weight  $e^{-\beta x/2}$ . These correspond to the Wishart matrices  $A_1 A_1^T$  with

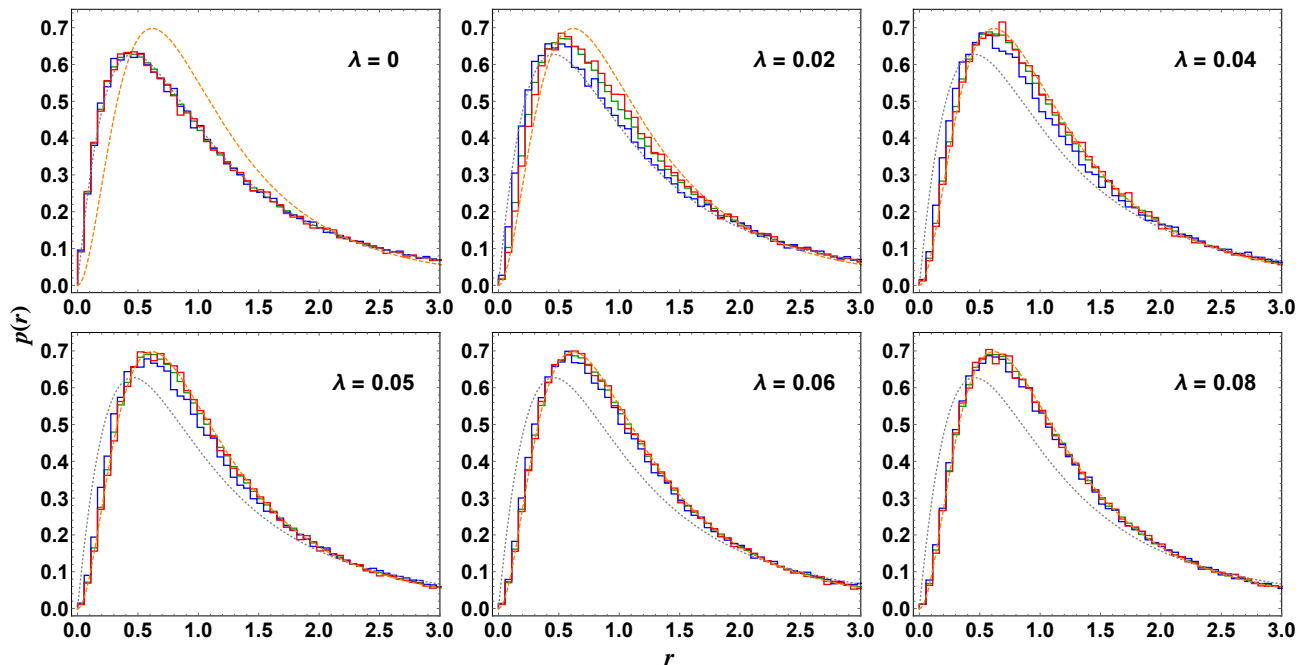


FIG. 3: Behavior of the ratio distribution computed using the middle part (red stairs), edges (blue stairs), and the entire spectrum (green stairs) for the GOE-GUE crossover.

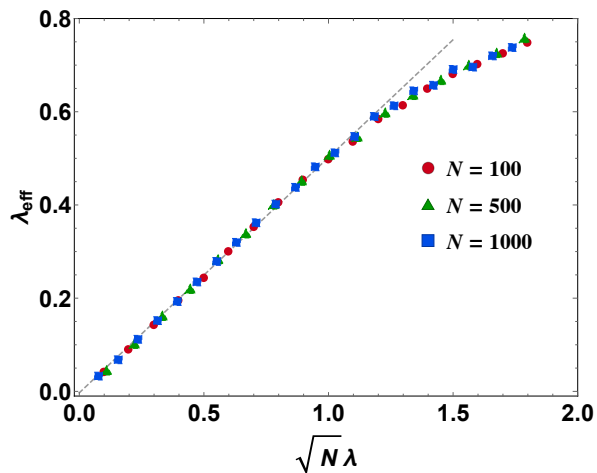


FIG. 4: Scaling behavior of the effective transition parameter  $\lambda_{\text{eff}}$  in the GOE-GUE crossover.

$N = 3, M = 4$  and  $A_2 A_2^\dagger$  with  $N = M = 3$ , and read

$$p_{\text{LOE}}(r) = 32 \frac{(r^2 + r)}{(r + 2)^5}, \quad (21)$$

$$p_{\text{LUE}}(r) = 420 \frac{(r^2 + r)^2}{(r + 2)^8}. \quad (22)$$

In the limits  $r \rightarrow 0$  and  $r \rightarrow \infty$ , the asymptotic behaviors of these functions are  $r^\beta$  and  $r^{-\beta-2}$ , respectively, which coincide with the corresponding asymptotic behaviors of

GOE and GUE results in Eqs. (16) and (18). However, overall shapes of these distributions based on  $3 \times 3$  cases of Laguerre and Gaussian ensembles are very distinct. For large  $N$ , we find that the empirical ratio distributions for the Laguerre ensemble are closely approximated by the Gaussian ensemble results instead of the above two equations. This is demonstrated in Fig. 5 where we plot the ratio distributions obtained from numerical simulation based on the above described Wishart-Laguerre matrix model. For comparison, we also plot the analytical expressions from Eqs. (16), (18), (21) and (22). We can see that for  $N = 500$ , the empirical ratio distributions for the Laguerre ensemble are well described by the Gaussian  $3 \times 3$  results, thereby affirming their universality.

We now analyze the LOE-LUE crossover. The matrix model implemented is

$$W = AA^\dagger, \quad (23)$$

where

$$A = \frac{1}{\sqrt{1 + \lambda^2}} A_1 + \frac{\lambda}{\sqrt{1 + \lambda^2}} A_2. \quad (24)$$

We focus on the large  $N = M$  case, for which the level density for the Wishart random matrix  $W$  is given by

$$R_1(x) = \begin{cases} \frac{1}{\pi} \sqrt{\frac{2N-x}{x}}, & 0 \leq x \leq 2N, \\ 0, & \text{otherwise.} \end{cases} \quad (25)$$

For the above LOE to LUE crossover ensemble, the effective transition parameter is known to be  $\lambda_{\text{eff}} \sim$

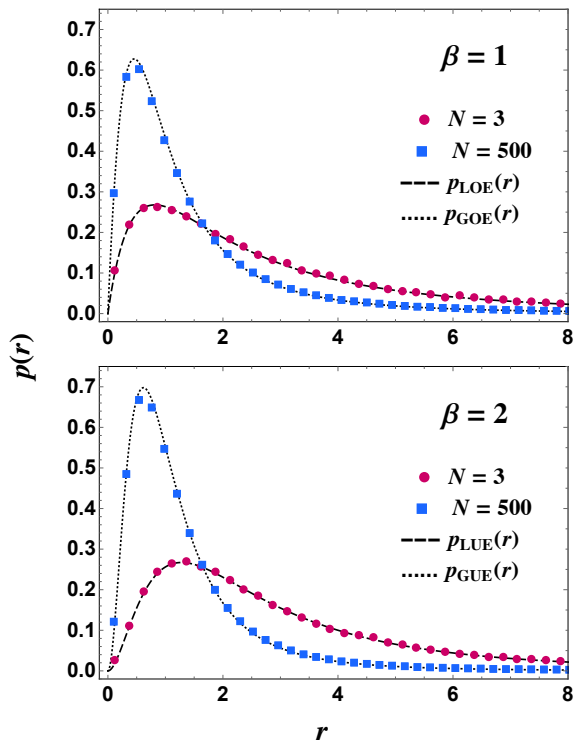


FIG. 5: Distribution of the ratio of two consecutive spacings in Laguerre orthogonal ( $\beta = 1$ ) and Laguerre unitary ( $\beta = 2$ ) ensembles.

$\lambda\sqrt{x}R_1(x) \sim \lambda\sqrt{2N-x}$  [33, 34, 44], which depends on the location in the spectrum. However, away from the right edge, we have  $\lambda_{\text{eff}} \sim \sqrt{N}\lambda$  and we expect this scaling to work for the the entire spectrum collectively, similar to the Gaussian case. We verify this with the aid of matrices generated using Eq. (23) for  $N = 500, 1000, 1500$  and varying  $\lambda$  values. The empirical ratio distributions are fitted with the formula in Eq. (15) to obtain the effective  $\lambda_{\text{eff}}$  and then plotted against  $\sqrt{N}\lambda$  in Fig. 6. The data points almost fall on a common line for small values of  $\lambda$ , which indicates validity of the above mentioned scaling for LOE-LUE crossover.

## VI. SYMMETRY CROSSOVER IN QUANTUM KICKED ROTOR

The quantum kicked rotor (QKR) was introduced to serve as a simple yet significant model to aid investigations into quantum chaos [43]. Since then QKR and its variants have been extensively used in several contexts [45–54]. The Hamiltonian for the kicked rotor system is given by

$$\mathcal{H} = \frac{(p + \gamma)^2}{2} + \alpha \cos(\theta + \theta_0) \sum_{n=-\infty}^{\infty} \delta(t - n). \quad (26)$$

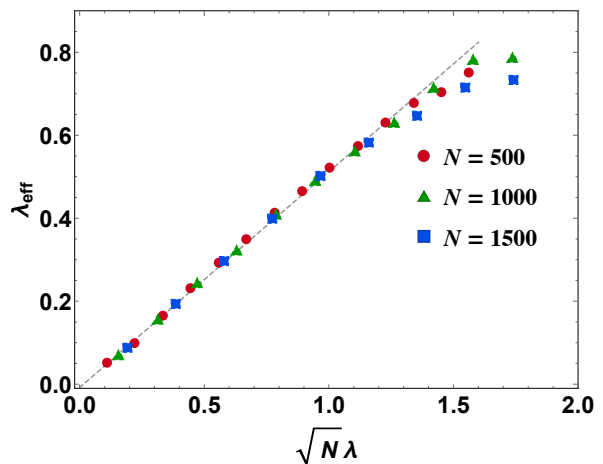


FIG. 6: Scaling behavior of the effective transition parameter  $\lambda_{\text{eff}}$  in the LOE-LUE crossover.

It describes a particle restricted to a ring and receiving position dependent periodic kicks. In the above equation  $p$  is the momentum operator,  $\theta$  is the position operator and  $\alpha$  is the stochasticity parameter. The role of the parameters  $\gamma$  is to imitate the effect of time-reversal breaking while  $\theta_0$  facilitates the parity violation. The periodic kicks at integer time instants ( $t = n$ ) is provided by the Dirac comb. The associated quantum dynamics may be described by the discrete time evolution operator (Floquet operator)  $U$  by imposing the torus boundary condition on the phase space. Considering the finite dimensional model, we obtain the evolution operator in position basis as [45, 46]

$$U_{mn} = \frac{1}{N} \exp\left[-i\alpha \cos\left(\frac{2\pi m}{N} + \theta_0\right)\right] \times \sum_{l=-N'}^{N'} \exp\left[-i\left(\frac{l^2}{2} - \gamma l + \frac{2\pi l(m-n)}{N}\right)\right]. \quad (27)$$

In the above summation,  $N'$  is  $(N-1)/2$  with  $N$  odd and  $m, n$  take the values  $-N', -N'+1, \dots, N'$ . A high degree of chaos is necessary for the spectral fluctuation properties of the QKR to correspond to classical RMT ensembles [45–47]. This can be achieved by assigning the parameter  $\alpha$  a very high value. For studying the violation of time-reversal invariance, we set  $\theta_0 = \pi/(2N)$  (fully broken parity symmetry) and then vary  $\gamma$  gradually. This leads the eigenangle (or eigenphase) spectrum of  $U$  to exhibit a transition from orthogonal to unitary class, which has been shown to be described very well using the crossover from Circular Orthogonal Ensemble (COE) to Circular Unitary Ensemble (CUE) [26, 48, 49]. In the following, we examine the crossover in the distribution of ratio of two consecutive eigenangles and dependence of the transition parameter  $\lambda_{\text{eff}}$  on the time-reversal violation parameter  $\gamma$ .

For our analysis, we consider  $N = 51, 101, 151$  and generate the corresponding ensembles of  $U$  matrices by

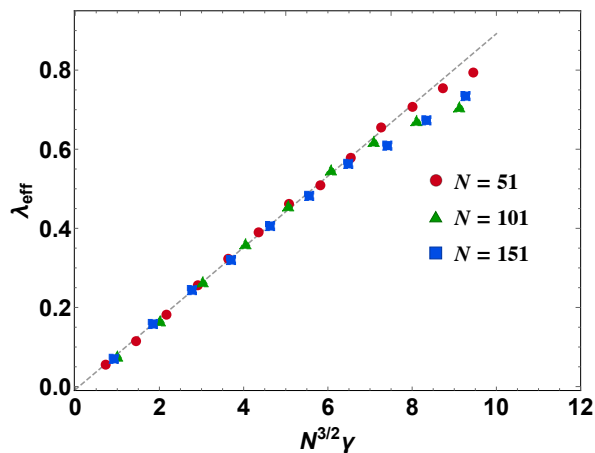


FIG. 7: Dependence of the effective crossover parameter  $\lambda_{\text{eff}}$  on the time-reversal violation parameter  $\gamma$  of QKR system.

varying the stochasticity parameter  $\alpha$  in the neighborhood of 20000. These matrices are diagonalized to obtain the eigenvalues which are of the form of  $e^{i\phi_j}$ , with  $\phi_j$  being the eigenangles. The eigenangles are uniformly distributed in  $[-\pi, \pi)$  and therefore the level density is  $R_1(\phi) = N/(2\pi)$ . It is also known based on a semiclassical analysis that the effective transition parameter  $\lambda_{\text{eff}}$  for this system is proportional to  $\gamma N^{3/2}$  [48, 49]. This is verified in Fig. 7 where we plot  $\lambda_{\text{eff}}$  versus  $\gamma N^{3/2}$ . The  $\lambda_{\text{eff}}$  values have been obtained by fitting the numerically obtained ratio distributions with Eq. (15). We observe linear behaviour for small values of  $\gamma$  which confirms the above relationship between  $\lambda_{\text{eff}}$  and  $\gamma$ .

## VII. SUMMARY AND OUTLOOK

For analyzing the spectral fluctuations of complex physical systems, distributions of nearest neighbor spac-

ing and their ratio are two widely used measures. The latter is convenient to apply since it circumvents the procedure of unfolding the spectrum. For the invariant classes, the ratio distributions were recently derived. These results are analogous to the Wigner surmise for the nearest neighbor spacing distributions. For the crossover ensembles, such as one describing a gradual time-reversal breaking, similar results are known for the nearest neighbor spacing distribution. However, similar results corresponding to the ratio of spacings have been missing. In this work, we aimed to fill this gap by deriving the Wigner surmise like result for ratio distribution in the orthogonal to unitary symmetry crossover. We also examined the proper scaling of the transition parameter which is needed to handle large size spectra by studying the Gaussian and Laguerre crossover ensembles. Additionally, we investigated the effect of time-reversal symmetry breaking in the spectrum of quantum kicked rotor by examining the behavior of ratio distribution of eigenangles and the associated scaling of the transition parameter.

Aside from the orthogonal-unitary crossover ensemble, there are several random matrix models which are useful in exploring other kinds of spectral transitions. For instance, the Poisson to Gaussian-ensemble crossover is useful in quantifying the transition from integrability to chaos. It would be of interest to see if similar universal results can be obtained for other crossover ensembles.

## ACKNOWLEDGMENTS

A. S. acknowledges DST-INSPIRE for providing the research fellowship [IF170612]. S.K. acknowledges the support by the grant EMR/2016/000823 provided by SERB, DST, Government of India.

- 
- [1] T. A. Brody, J. Flores, J. B. French, P. A. Mello, A. Pandey and S. S. M. Wong, *Rev. Mod. Phys.* **53**, 385 (1981).
  - [2] G. E. Mitchell, A. Richter, and H. A. Weidenmüller, *Rev. Mod. Phys.* **82**, 2845 (2010).
  - [3] L. Laloux, P. Cizeau, J-P. Bouchaud and Marc Potters, *Phys. Rev. Lett.* **83**, 1467 (1999).
  - [4] V. Plerou, P. Gopikrishnan, B. Rosenow, L. A. Nunes Amaral, and H. Eugene Stanley, *Phys. Rev. Lett.* **83**, 1471 (1999).
  - [5] R. N. Mantegna and H. E. Stanley, *An Introduction to Econophysics: Correlations and Complexity in Finance* (Cambridge University Press, Cambridge, UK, 1999).
  - [6] A. M. Tulino, S. Verdú and A. M. Tulino, *Random Matrix Theory and Wireless Communications (Foundations and Trends in Communications and Information)*, vol. 1. (Now Publishers, Delft, The Netherlands, 2004).
  - [7] R. Couillet and M. Debbah, *Random Matrix Methods for Wireless Communications* (Cambridge University Press, Cambridge, UK, 2011).
  - [8] S. Kumar and A. Pandey, *IEEE Trans. Inf. Th.* **56**, 2360 (2010).
  - [9] C. W. J. Beenakker, *Rev. Mod. Phys.* **69**, 731 (1997).
  - [10] C. W. J. Beenakker, *Rev. Mod. Phys.* **87**, 1037 (2015).
  - [11] M. L. Mehta, *Random Matrices* (New York: Academic Press, 2004).
  - [12] T. Guhr, A. Müller-Groeling and H. A. Weidenmüller, *Phys. Rep.* **299** **4**, 189 (1998).
  - [13] P. J. Forrester, *Log-Gases and Random Matrices (LMS-34)* (Princeton University Press, 2010).
  - [14] F Haake, *Quantum Signatures of Chaos* (Springer, New York, 2010).

- [15] G. Akemann, J. Baik, and P. Di Francesco (eds.), *Handbook of Random Matrix Theory* (Oxford Press, 2011).
- [16] O. Bohigas, M. J. Giannoni, and C. Schmit, *Phys. Rev. Lett.* **52**, 1 (1984).
- [17] Y. Y. Atas, E. Bogomolny, O. Giraud, and G. Roux, *Phys. Rev. Lett.* **110**, 084101 (2013).
- [18] Y. Y. Atas, E. Bogomolny, O. Giraud, P. Vivo, and E. Vivo, *J. Phys. A: Math. Theor.* **46**, 355204 (2013).
- [19] M. Berry and M. Tabor, *Proc. R. Soc. A* **356**, 375 (1977).
- [20] F. J. Dyson, *J. Math. Phys.* **3**, 1199 (1962).
- [21] F. J. Dyson, *J. Math. Phys.* **13**, 90 (1972).
- [22] A. Pandey and M. L. Mehta, *Commun. Math. Phys.* **87**, 449 (1983).
- [23] M. L. Mehta and A. Pandey, *J. Phys. A: Math. Gen.* **16**, 2655 (1983).
- [24] G. Lenz and Fritz Haake, *Phys. Rev. Lett.* **65**, 2325 (1991).
- [25] G. Lenz, K. Życzkowski, and D. Saher, *Phys. Rev. A* **44**, 8043 (1991).
- [26] A. Pandey and P. Shukla, *J. Phys. A: Math. Gen.* **24**, 3907 (1991).
- [27] A. Pandey, *Ann. Phys. (N.Y.)* **134**, 110 (1981).
- [28] J. B. French, V. K. B. Kota, A. Pandey, and S. Tomsovic, *Ann. Phys.* **181**, 198 (1988).
- [29] T. Guhr, *Ann. Phys.* **250**, 145 (1996).
- [30] S. Schierenberg, F. Bruckmann, and T. Wettig, *Phys. Rev. E* **85**, 061130 (2012).
- [31] P. J. Forrester, T. Nagao and G. Honner, *Nucl. Phys. B* **553**, 601 (1999).
- [32] T. Nagao and P. J. Forrester, *Nucl. Phys. B* **660**, 557 (2003).
- [33] S. Kumar and A. Pandey, *Phys. Rev. E* **79**, 026211 (2009).
- [34] S. Kumar and A. Pandey, *Ann. Phys.* **326**, 1877 (2011).
- [35] N. D. Chavda, H. N. Deota, and V. K. B. Kota, *Phys. Lett. A* **378**, 3012 (2014).
- [36] F. Schweiner, J. Laturner, J. Main and G. Wunner, *Phys. Rev. E* **96**, 052217 (2017).
- [37] F. Schweiner, J. Main and G. Wunner, *Phys. Rev. E* **95**, 062205 (2017).
- [38] P. Braun, S. Heusler, S. Müller, and F. Haake, *J. Phys. A: Math. Gen.* **39**, L159 (2006).
- [39] B. Béri and J. Cserti, *Phys. Rev. B* **75**, 041308 (2007).
- [40] K. Frahm and J.-L. Pichard, *J. Physique (I)* **5** 847 (1995).
- [41] S. Kumar and A. Pandey, *J. Phys. A: Math. Th.* **43**, 285101 (2010).
- [42] S. Kumar and A. Pandey, *J. Phys. A: Math. Th.* **43**, 085001 (2010).
- [43] G. Casati, B. Chirikov, J. Ford and F. M. Izrailev, *Stochastic Behavior in Classical and Quantum Hamiltonian Systems*, in *Lecture Notes in Physics*, Vol. 93, p. 334, edited by G. Casati and J. Ford (Springer-Verlag, Berlin, 1979).
- [44] The effective crossover parameter in Refs. [33, 34] is  $\lambda_{\text{eff}} \sim \sqrt{x\tau}R_1(x)$  where  $\tau$  is the crossover parameter used therein. It relates to the parameter  $\lambda$  used here as  $\tau = \ln(1 + \lambda^2)$ . For small values of the crossover parameter,  $\tau \approx \lambda^2$ , which gives  $\lambda_{\text{eff}} \sim \sqrt{x}\lambda R_1(x)$ .
- [45] F. M. Izrailev, *Phys. Rev. Lett.* **56**, 541 (1986).
- [46] G. Casati, I. Guarneri, F. Izrailev, and R. Scharf, *Phys. Rev. Lett.* **64**, 5 (1990).
- [47] F. M. Izrailev, *Phys. Rep.* **196**, 299 (1990).
- [48] A. Pandey, R. Ramaswamy and P. Shukla, *Pramana* **41**, 75 (1993).
- [49] P. Shukla and A. Pandey, *Nonlinearity* **10**, 979 (1997).
- [50] A. Lakshminarayan, *Phys. Rev. E* **64**, 036207 (2001).
- [51] S. C. L. Srivastava and A. Lakshminarayan, *Chaos, Solitons & Fractals* **74**, 67 (2015).
- [52] A. Pandey, A. Kumar, and S. Puri, *Phys. Rev. E* **96**, 052211 (2017).
- [53] A. Kumar, A. Pandey, and S. Puri, arXiv:1905.10530 (2019).
- [54] A. B. Jaiswal, R. Prakash, and A. Pandey arXiv:1904.12484 (2019).